MECHANIKA TEORETYCZNA
I STOSOWANA
Journal of Theoretical
and Applied Mechanics
4, 33, 1995

ON THE DESIGN OF INTERFERENCED AND CLAMPED JOINTS UNDER GENERAL STATE OF STRESS

JERZY OSIŃSKI

ANDRZEJ SZTWIERTNIA

Institute of Machine Design Fundamentals

Warsaw University of Technology

Problems arising in the case of assuming general stress state in the interferenced joint are considered in this paper. FEM program using sensitivity matrix method written by the authors has been used for the analysis of non-linear contact problems (cf Osiński and Sztwiernia (1994)). It includes non-linear characteristics of the stress-strain dependence that allows calculation of pre-plasticity of rough surfaces and plasticity. Full stress cycle has been applied to the joint; i.e., loading, unloading, loading. The results made it possible to plot the hysteresis loop. In particular the analysed issues are the effect of boundary conditions (bush attachment) and joint dimensions. Big difference has been highlighted between authors' results and the ones obtained for simplified models for short joints of big diameter. The hysteresis loop is shifted and its area is much bigger. The influence of contact pressure increase in the edge area was also considered. An analytical method was also developed. The influence of pressure increase has small effect on energy dissipation.
It has been stated that in the analysis of contact problems with friction (structural damping) the use of general state of stress is recommended. The uniaxial torsion assumption is a great simplification. The FEM program using the sensitivity matrix method turned out to be a very efficient tool in the analysis of contact problems.

1. Introduction

In methods currently used for the design of interferenced and clamped joints numerous simplifications are made. Therefore the general stress state occurring in these joints is discarded. Particularly, in the case of interferenced joints, the formulas arising from Lamé's strain potential are used, with plastic strains taken into account, cf textbooks on joints: Krukowski and Tutaj

(1987), Porębska (1991). There are also numerous works devoted to comple problems; e.g., consideration of mixed characteristics (friction and elasticity in tangent contact (Grudziński and Konowalski (1989), (1991), (1993)), or th problem of energy dissipation in the joint (Osiński (1986)). Models used in th aforementioned works are relatively simple (geometrically). The uniform d stribution of pressure on the surface of the bodies being in contact is assume or uniaxial state of stress is considered.

The aim of this paper is to analyse the phenomena revealed when con plex, 2- or 3-axial state of stress is assumed. In particular, the analysed issue are the effect of boundary conditions (bush attachment), joint dimensions an non-uniformity of pressure distribution (the increase in the edge area). Appl cation of the finite elements approach to this problem made the exact analys possible. The calculations were carried out for axisymmetric interferenced an clamped joints with torsional load applied. A computer program drawn up b the authors exploiting the concept of sensitivity matrix has been used. Th program, described by Osiński and Sztwiernia (1994), can be used for analys of non-linear contact problems. The non-linear approach gives consideratio to roughness and pre-plasticity on the contact surface. Full stress cycle ha been applied to the joint; i.e., loading, unloading, loading. The results mad it possible to plot the hysteresis loop.

2. Model of the joint

A computational model of axisymmetric joint, as shown in Fig.1a, has bee assumed. The model describes various interferenced and clamped joints. Th evaluation process (algorithm) is the same, only the iteration end condition are different. These are contact pressure values for given external load, bo tension or negative allowance. Various types of boundary conditions dependin on the bush attachment method can be imposed.

Ultimately, exploiting the advantages of model's symmetry, the three typ of boundary conditions were obtained. These are shown in Fig.2.

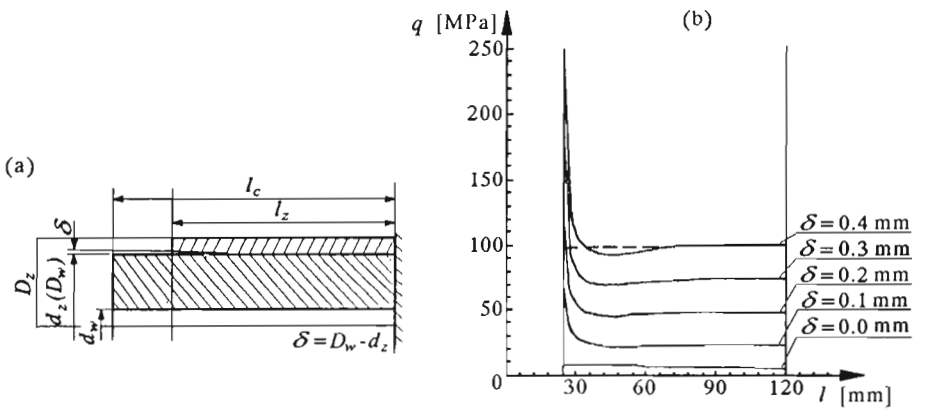

Fig. 1. Assumed computational model and the distribution of contact stress against the pressure in the interferenced joint

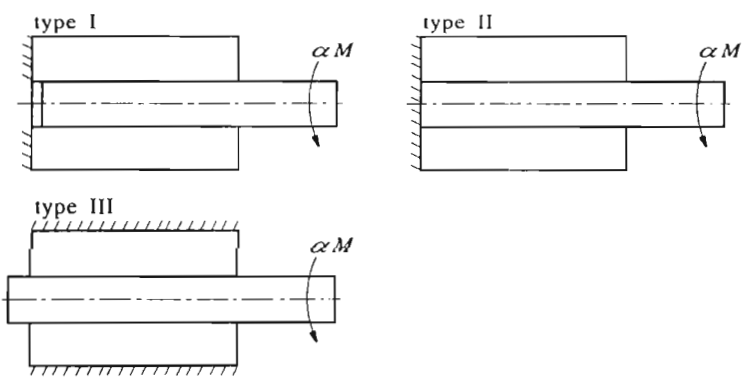

Fig. 2. Boundary conditions

The numerical calculations were carried out for the set of data given in Table 1.

Table 1

Outer bush diameter	$D_z = 180\,\text{mm}$
Inner bush diameter, outer shaft diameter	$D_{wm} = d_{zm} = 140\,\text{mm}$
Inner shaft diameter	$d_w = 80\,\text{mm}$
Elastic modulus (for bush and shaft)	$E = 210000\,\text{MPa}$
Poisson ratio (for bush and shaft)	$\nu = 0.33$
Coefficient of friction	$\mu = 0.4$
Roughness parameter	$R_a = 30\,\text{mm}$
Contact stiffness normal to the surface	$C_N = 105000\,\text{MPa}$
Initial gap in clamped joint	$z = 0.4\,\text{mm}$
Joint length	in each case assumed for the obtained length/diameter ratio

A complex model of contact has been assumed. The phenomena of dry friction (Coulomb friction) and roughness, including its closure under load, have been taken into account. The phenomena occurring on the contact surface of two bodies are complicated in result of:

- Random distribution of surface shape deviation
- Physical changes of the surface (partial plasticity of the upper layer)
- The occurrence of impurities, oxides.

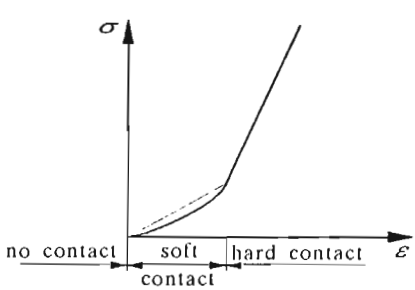

Fig. 3. Normal contact characteristic

In computational methods (e.g. FEM) a characteristics of contact shown in Fig.3 has been assumed. Its non-linear part describes the soft contact. The physical changes occur in the upper layer for this strain range. These changes are: plasticity, strengthening and crack closure. The characteristic is approximated with the exponential function. The other part of the characteristic – hard contact – is drawn according to Hooke's law.

If the range of the soft contact is narrow this part of the characteristic can be approximated with a straigth line as shown in Fig.3. This simplification results in sufficient accuracy of the result and it simplifies programming.

The material data obtained from other sources have been cross-checked with experimental studies carried out in the rheological laboratory of Institute of Machine Design Fundamentals Warsaw University of Technology. The results obtained for steel with rough surface (after turning), steel with smooth surface (after grinding) and plastics – polyamid are marked 1, 2, 3, respectively, and shown in Fig.4.

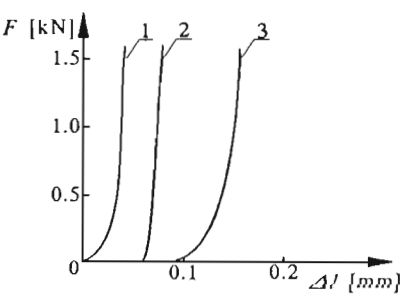

Fig. 4. Experimentally obtained normal contact characteristic

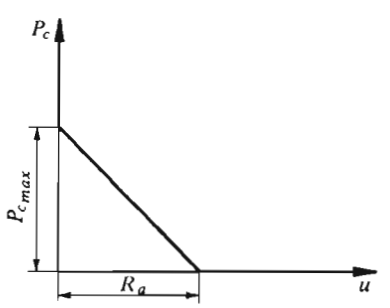

Fig. 5. Normal contact characteristic in the (u, P_c) coordinates

It can be seen that the area of soft contact for steel is relatively small and its width is connected with the surface roughness. Therefore it can be assumed

that the contact deflection area is equivalent to the roughness area. Thus the $\sigma - \varepsilon$ relationship can be approximated with two straigth lines as shown in Fig.3.

This characteristic has been transformed to the (u, P_c) coordinates as shown in Fig.5. The latter is easier to implement into the computer program.

3. Acceleration of iteration process by means of sensitivity matrix

The calculation of contact problems is carried out on the basis of the following algorithm:

- Description of both structures being in contact is generated, the initial spacing is described by linear model, stiffness matrices $\mathbf{K}_1$ and $\mathbf{K}_2$ are calculated
- The nodes on the contact surfaces (values of functions) are stored in memory (gap nodes)
- The overall structure stiffness matrix is created in the form

$$\mathbf{K} = \begin{bmatrix} \mathbf{K}_1 & 0 \\ 0 & \mathbf{K}_2 \end{bmatrix} \tag{3.1}$$

  and the inverse of it is constructed
- Sensitivity matrix is created by sequential introducing unit loads normal to the contact surface in all nodes; and the inverse of this matrix is constructed
- External pressure is introduced, the values of displacements are calculated and, depending on the gap value, one of the next steps is performed:
  - If the value of the gap is greater than the roughness parameter (no contact), the next pressure value is taken
  - If the value of the gap is smaller than the roughness parameter (soft contact), certain value of contact pressure is assumed and iteration process is continued until the former gap value is obtained
  - If the value of the gap is negative (hard contact) the contact pressure value is assumed and iteration process is continued until the zero gap is obtained

– In the case of forced-in joint the iteration process is continued until the zero gap value is reached.

If the friction is to be introduced an additional sensitivity matrix for tangent forces is created – iterations for these forces are performed within each step for normal forces. The mitigated solid friction must not be exceeded at any node on the contact surface.

When external forces other than those arising from interference or clamp, are employed, the calculations for subsequent nodes are made with different force values. The values of fixed displacements are taken from the system under the previous load ("a system with memory").

4. Joint dimensions

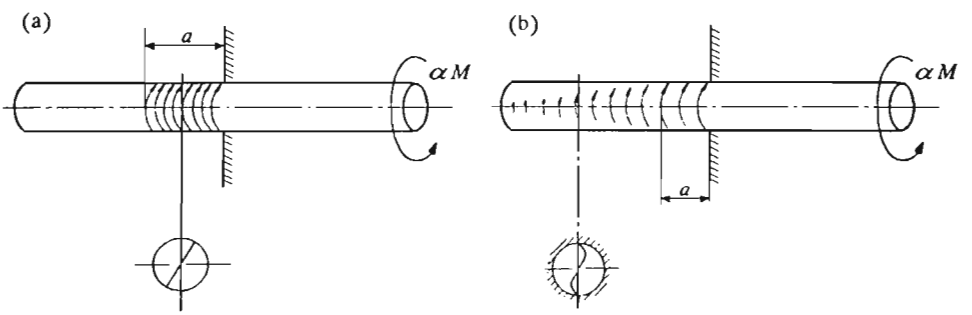

Fig. 6. Explanation of the influence of joint dimension in the case of torsional load

In the analysis of general stress state the length/diameter ratio for the joint plays an important role. The explanation of the influence of this ratio is shown in Fig.6. In Fig.6a only uniaxial torsion is applied to the joint. The slip zone of length a, with developed friction can be observed. The cross-section with strains (deflections) indicated is shown in Fig.6b. Neither strain nor stress can be observed in the other part of the joint. In the case of more complex (2-axial) state of stress the slip zone is shorter, while in the other part of the joint the stiction phase occurs. It is the result of the strain (deflection) close to the attached edge. Similar character of this phenomenon can be observed in the case of axial load.

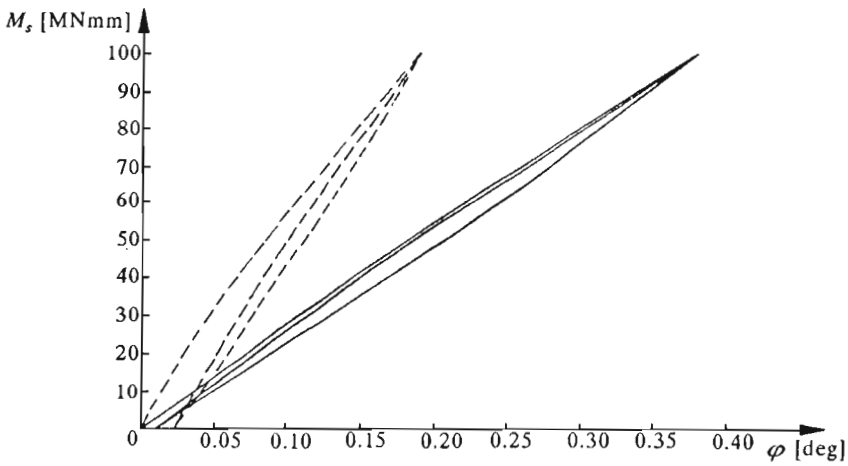

Fig. 7. Hysteresis loop for the joint with $l_z = 200\,\text{mm}$

The hysteresis loop shown in Fig.7 is a result of FEM calculations of a clamped joint with the contact pressure

$$q = 95.7\ \text{MPa} \tag{4.1}$$

and joint length

$$l_z = 200\ \text{mm} \tag{4.2}$$

The l_z/D ratio is thus 1.43, the boundary conditions are of type I. The area of the hysteresis loop (the amount of energy dissipated) is

$$\psi_{FEM} = 17\ \text{Nm} \tag{4.3}$$

For comparison the hysteresis loop obtained according to the formulas given by Osiński (1986) has been drawn with the dotted line. The numerical values were calculated with the aid of the program for joint design presented by Osiński (1994). It can be clearly seen that the hysteresis loop is shifted. Greater torsion angles occur for the same loads. The area of the loop is smaller

$$\psi_T = 13\ \text{Nm} \tag{4.4}$$

Similar dependency was observed in other cases analysed by the authors for broader dimension range.

The results are presented in Fig.8 as the ratios of loop areas (FEM and theoretical)

$$i_\psi = \frac{\psi_{FEM}}{\psi_T} \tag{4.5}$$

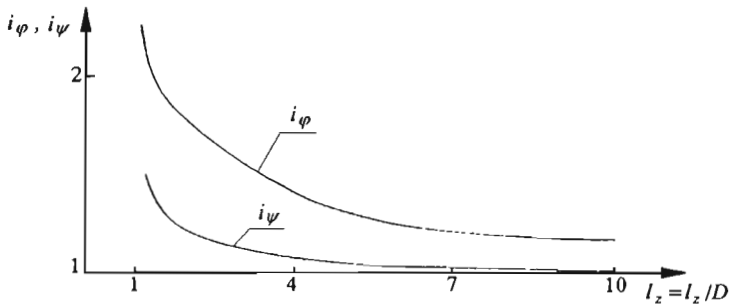

Fig. 8. Dependence of the loop area and torsion angle on the joint dimension

and the maximal torsion angles

$$i_\varphi = \frac{\varphi_{FEM}}{\varphi_T} \tag{4.6}$$

respectively. Both curves were plotted against the length/diameter ratio. As it can be observed, the shorter and broader the joint is, the bigger the difference between the theoretical and authors' results. For longer and narrower joints the authors' results and the ones obtained by Osiński (1986) are much closer to each other. Qualitatively similar effect was obtained for flat clamped joints. The shift of the loop and the increase of its area is shown in Fig.9 (taken from Osiński (1984)). The loop plotted with solid line was obtained using the method described here.

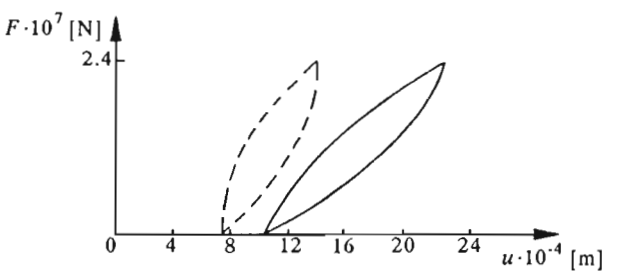

Fig. 9. Hysteresis loop in the joint under axial load

The results obtained, particularly the increase in the torsion angle, are of great importance. They can be used for the evaluation of stiffness of the joints in power transmission systems of machine tools. The "FEM stiffness" can be different from the value calculated according to the formulas given by

Marchelek (1991). For a great complexity of this problem it will be described in another paper.

5. Load application mode

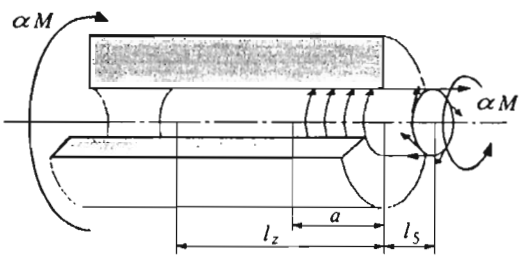

Fig. 10. Distribution of tangent forces

When the length of the free end of the joint is small the way in which the load is applied is important. The Saint-Venant principle can not be employed in this case. The calculations have been made for tangent forces distributed over the edge, as shown in Fig.10. For the long free end of the joint the load is equivalent to the torsional moment. The hysteresis loop area is thus

$$\psi = 17.5 \text{ Nm} \tag{5.1}$$

For the short free end ($d_S = 10\,\text{mm}$) the stress distribution in the joint is different, and the hysteresis loop area is

$$\psi = 9 \text{ Nm} \tag{5.2}$$

and is smaller by 50%. The comparison of both loops is shown in Fig.11 (solid line – (9), dotted line – (10)).

6. Boundary conditions – bush attachment

The simplified theoretical models can be used only when boundary conditions bear out the assumption of uniaxial state of stress. These are types I and II as shown in Fig.2. In other cases the results can be obtained only

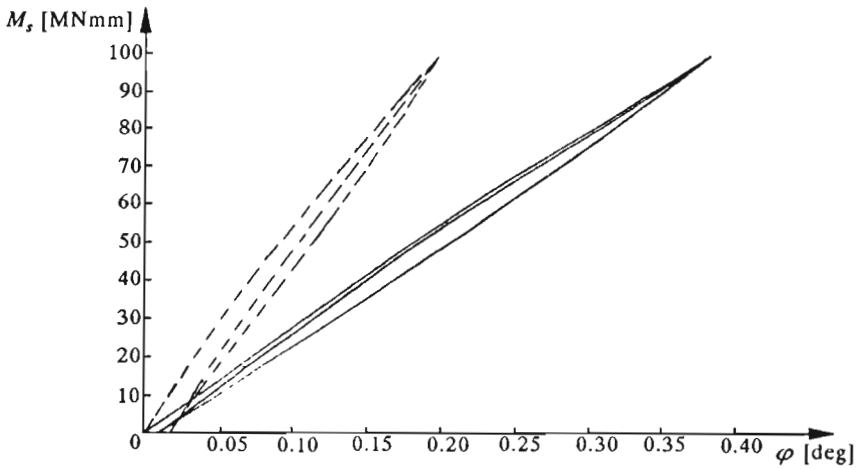

Fig. 11. Hysteresis loop in the joint with short free end

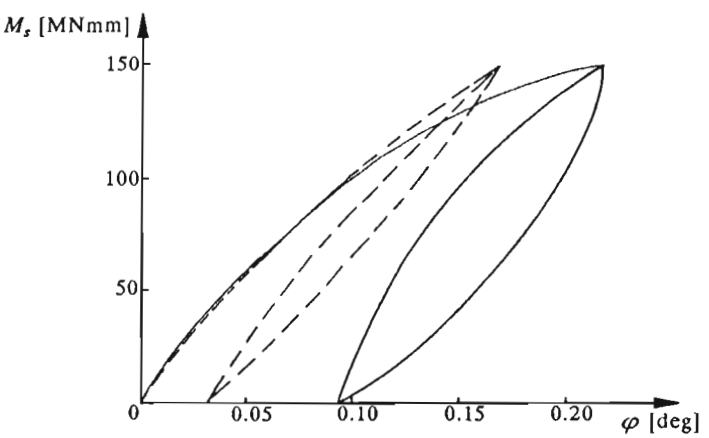

Fig. 12. Hysteresis loop in the joint under the boundary conditions of type III

with the FEM. This is the case of boundary condition of type III. The hysteresis loop shown in Fig.12 was calculated with the aid of authors' program for interferenced joint. The interference was chosen to obtain the contact pressure

$$q = 140 \text{ MPa} \tag{6.1}$$

The loop plotted with dotted line was calculated using theoretical formulas for the boundary conditions of type I. It can be seen that the loop is shifted and its area is much bigger. It happened because the boundary conditions of type III affect the increase of the stiffness of the bush. In the case of the stiff bush the way of attachment is not important. All boundary conditions are the same. Practically this simplification is acceptable when the bush stiffness is much greater than the shaft stiffness. It is the case when the coefficient

$$k = \frac{GI}{GI + G_1 I_1} \tag{6.2}$$

tends to 0. In this formula G is the Kirchhoff modulus, I is the moment of inertia, index 1 describes bush, no index – shaft.

7. The phenomenon of contact pressure increase in the edge area

The contact pressure distribution in the joint is not uniform. Particularly important is the pressure distortion in the edge area. The stress increases there in result of the boundary conditions influence. Establishing of the exact value of pressure is extremely difficult due to the stress concentration. The pressure values vary considerably on a relatively small area. A special type of finite elements must be adopted to allow estimation of the accuracy. These are semi-analytic elements or adaptive systems. When the typical FEM system is used a great number of finite elements are necessary (coarse mesh) in the stress concentration area. It considerably lengthens the calculation time. The yield point can be also exceeded in the edge area, as it was shown by Buczkowski and Kleiber (1992). The effect of the pressure increase in the edge area has been corroborated in numerous experimental and theoretical works.

Closer inspection of the results shown in Fig.1b shows that the shorter the joint is the bigger increase can be observed. A similar phenomenon occurs for bigger external load and greater value of allowance.

The problem of increased contact pressure in the edge area influence on the energy dissipation in interferenced joints (structural damping) has not been yet examined. That was the aim of this work.

7.1. Theoretical analysis

The investigation of structural damping was conducted using the method presented by Osiński (1986). All assumptions expressed there were accepted. The additional assumption regarding the pressure distribution was propounded. It was approximated with two constant levels as shown with dotted line in Fig.13. For each level formulas given by Osiński (1986) were used. The length of the first zone is always the same (the value of a_k in Fig.13). The end values for this zone are the initial conditions for the other one.

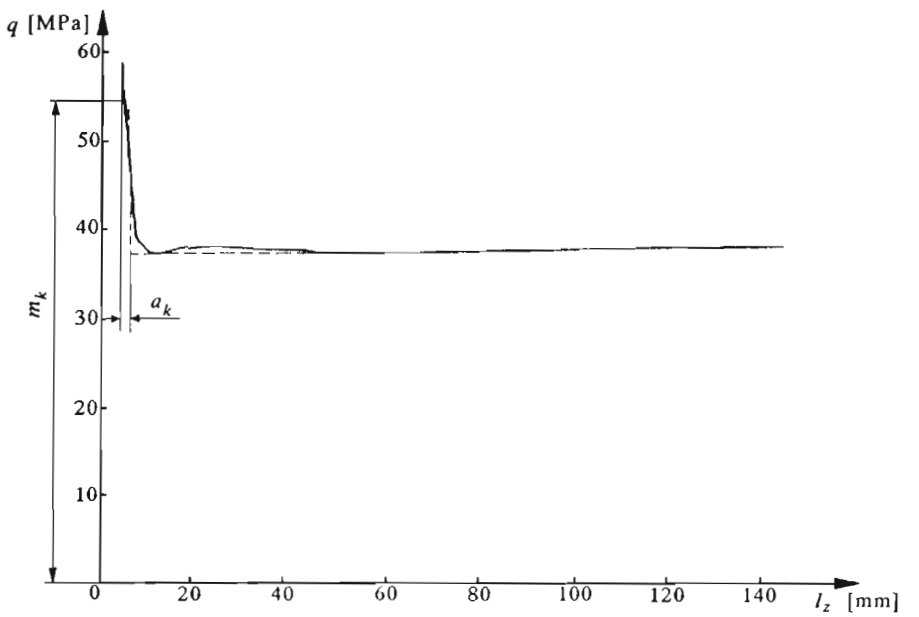

Fig. 13. Approximation of pressure distribution

The calculations are made on the basis of the following algorithm:

- Step 1 – loading

— calculating of torsional moment in the first zone

$$M_{1a} = a_k m_k \tag{7.1}$$

— torsion angle at the end of this zone

$$\varphi_{1a} = \frac{K_1}{2m_k GI}\alpha_{1a}^2 M_{1a}^2 + \frac{kl}{GI}\alpha_{1a} M_{1a} \tag{7.2}$$

— torsion angle at the end of second zone, step 1 end

$$\varphi_{1l} = \varphi_{1a} + \frac{K_1}{2mGI}(\alpha M - M_{1a})^2 + \frac{kl}{GI}(\alpha M - M_{1a}) \tag{7.3}$$

• Step 2 – unloading

— calculating of torsional moment at the end of the first zone

$$M_{2a} = 2a_k m_k \tag{7.4}$$

— torsion angle at this point

$$\varphi_{2a} = \frac{K_1}{4m_k GI}(1 + 2\alpha_{2a} - \alpha_{2a}^2) + \frac{\alpha_{2a} kMl}{GI} \tag{7.5}$$

— torsion angle

$$\varphi_{2l} = \frac{K_1}{4mGI}(1 + 2\alpha - \alpha^2) + \frac{\alpha kMl}{GI} \tag{7.6}$$

• Step 3 – loading

— calculating of torsional moment at the end of the first zone

$$M_{3a} = a_k m_k \tag{7.7}$$

— torsion angle at this point

$$\varphi_{3a} = \frac{K_1}{4m_k GI}(1 + 2r + \alpha_{3a}^2 - 2r\alpha_{3a}) + \frac{\alpha_{3a} kMl}{GI} \tag{7.8}$$

— torsion angle at the end of the second zone, step 3 end

$$\varphi_{3l} = \frac{K_1}{4mGI}(1 + 2r + \alpha^2 - 2r\alpha) + \frac{\alpha kMl}{GI} \tag{7.9}$$

where

m – elementary torsional moment
m_k – elementary torsional moment in the edge area
l – joint length
α, r – coefficients $< 0, 1 >$
K_1 – coefficient describing boundary conditions

$$K_1 = \begin{cases} \dfrac{1 - 3k + 3k^2}{1 - k} & \text{for type I} \\ 1 - k^2 & \text{for type II} \end{cases} \tag{7.10}$$

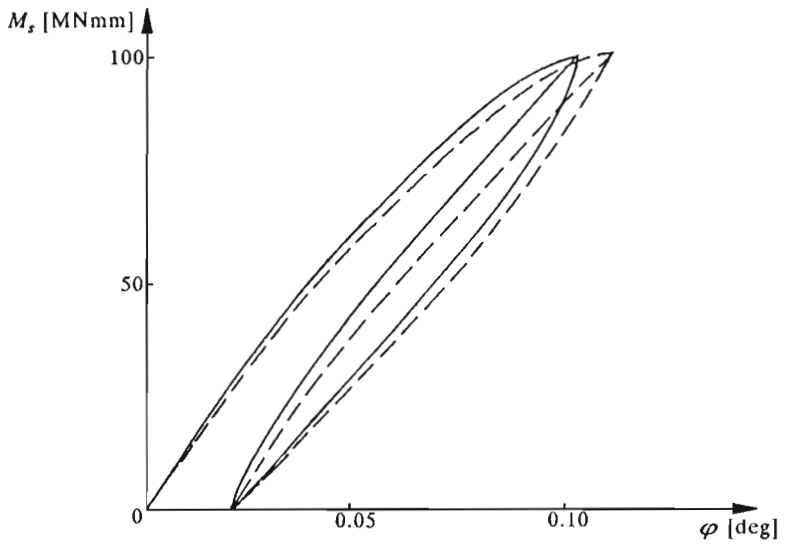

Fig. 14. Hysteresis loop for the joint with the increase of pressure in the edge area taken into account – the simplified model

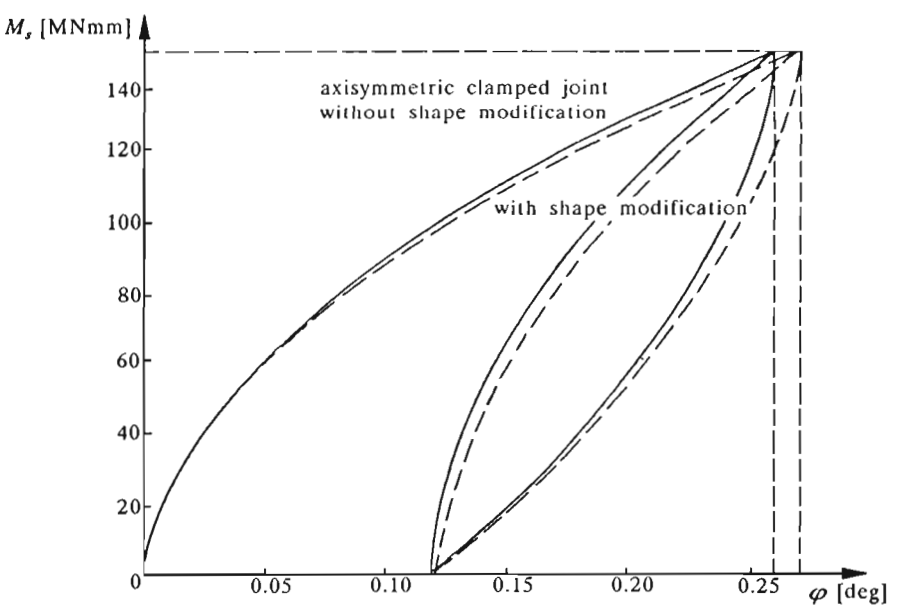

Fig. 15. Hysteresis loop for the joint with the increase of pressure in the edge area taken into account and with shape modification – the FEM model

The hysteresis loop presented in Fig.14 was drawn for joint with dimensions given in Table 1. The increase of pressure in the edge area has been taken into account (solid line) or has been omitted (dotted line). The difference between loop areas is small. The application of the aforementioned solution due to the simplifying assumptions accepted by Osiński (1986) is rather limited. More exact analysis requires the use of FEM.

7.2. FEM analysis

FEM program has been used when investigating the problems mentioned so far. For comparative reasons, the computations have been performed for joint with modified shape. The modification was meant to diminish significantly the values of stresses at the edges. The example (presented earlier by Osiński and Sztwiernia (1994)) is shown in Fig.15. The FEM analysis results confirm those arising from the theoretical analysis.

8. Conclusions

It has been shown that in the analysis of contact problems with friction (structural damping) it is necessary to consider the general state of stress. The uniaxial torsion assumption should be refuted. The dimensions of the joint (length/diameter ratio) have considerable influence on the energy dissipation effect. Big difference has been stated between authors' results and the ones obtained for simplified models for short joints with big diameter. The hysteresis loop is then shifted and its area is larger. The influence of pressure increase in the edge area on the energy dissipation is small. Also the influence of boundary conditions has been investigated. The FEM program using the sensitivity matrix method turned out to be a very efficient tool in the analysis of contact problems.

References

1. BUCZKOWSKI R., KLEIBER M., 1992, Finite Element Analysis of Elastic-Plastic Plane Contact Problem with Non-Linear Interface Compliance, *Journal of Theoretical and Applied Mechanics*, 30, r, Warsaw, 855-884

2. GRUDZIŃSKI K., KONOWALSKI K., 1989, Computer Aided Design of Clamped Joints, *VII-th Conference "CAD Methods"*, Warsaw, 98-105 (in Polish)

3. GRUDZIŃSKI K., KONOWALSKI K., 1991, Design of flat Clamped Joint with Contact Susceptibility, *Journal of Theoretical and Applied Mechanics*, **29**, 3-4, Warsaw, 605-620 (in Polish)

4. GRUDZIŃSKI K., KONOWALSKI K., 1993, Determining of Stresses, Strains and Local Slip Zones in Interferenced Joints under Torsional Load, *Archives of Mechanical Engineering and Automatization*, **12**, Poznań-Szczecin, 515-537 (in Polish).

5. KRUKOWSKI A., TUTAJ J., 1987, *Interferenced Joints*, PWN Warsaw (in Polish)

6. MARCHELEK K., 1991, *Dynamics of Machine Tools*, WNT Warsaw (in Polish)

7. OSIŃSKI J., 1984, The Application of Finite Elements Method to the Static Analysis of Connections with Structural Damping, *Proceedings of IPBM PW*, **14**, 133-150 (in Polish)

8. OSIŃSKI J., SZTWIERTNIA A., 1994, Modelling of Non-Linear Problems by Means of Sensitivity Matrix Method, *Machine Dynamics Problems*, 9, 71-82

9. OSIŃSKI Z., 1986, *Damping of Mechanic Vibrations*, PWN, Warsaw (in Polish)

10. OSIŃSKI J. EDIT., 1994, *Computer Aided Design of Typical Machine Elements*, PWN, Warsaw (in Polish)

11. PORĘBSKA M. (EDIT.), 1991, *Computer Aided Design of Machine Elements. Examples*, AGH Cracow (in Polish)

Obliczanie połączeń wciskowych i zaciskowych z uwzględnieniem złożonych stanów naprężeń

Streszczenie

W pracy zbadano problemy występujące w przypadku przyjęcia w obliczeniach połączeń nieruchomych złożonych stanów naprężeń. W analizie zastosowano własny program metody elementów skończonych wykorzystujący koncepcję macierzy wrażliwości do obliczeń nieliniowych zagadnień kontaktowych omówiony szczegółowo w poprzedniej pracy autorów z 1994r. W metodzie przyjęto nieliniowy charakter kontaktu uwzględniający chropowatość powierzchni i wstępne uplastycznienie powierzchni kontaktu. Wykonano pełne cykle obciążeń: obciążanie, odciążanie i ponowne obciążanie co umożliwilo wyznaczenie pętli histerezy. Rozważono wpływ warunków brzegowych (sposobu zamocowania tuleji) i wymiarów połączenia. Stwierdzono, że znaczne różnice między rozwiązaniami otrzymanymi w pracy a wynikami analizy uproszczonych modeli występują w przypadku połączeń krótkich o dużej średnicy – pętla histerezy jest przesunięta, a jej powierzchnia jest znacznie większa. Zbadano również wpływ wzrostu nacisków kontaktowych w pobliżu krawędzi połączenia – opracowano metodę analityczną i porównano z obliczeniami MES. Stwierdzono, że wzrost nacisków kontaktowych w pobliżu krawędzi połączenia ma nieznaczny wpływ na rozpraszanie energii w połączeniu.

Stwierdzono więc, że w analizie problemów kontaktowych z uwzględnieniem sił tarcia (zagadnienia tarcia konstrukcyjnego) konieczne jest przyjmowanie złożonych stanów naprężeń – założenie o występowaniu jednoosiowego skręcania jest znacznym przybliżeniem. Opracowana metoda obliczania zagadnień kontaktowych za pomocą elementów skończonych jest bardzo efektywnym (w wielu wypadkach praktycznie jedynym) sposobem analizy takich zagadnień.

Manuscript received July 5, 1994; accepted for print April 3, 1995